

Experimental Determination of the Static Equivalent Pressures of Detonative Explosions of Cyclohexane/O₂/N₂-Mixtures in Long and Short Pipes (part 2 of 3)

Hans-Peter Schildberg*, Julia Eble

BASF SE, 67056 Ludwigshafen, Germany
hans-peter.schildberg@basf.com

The abstract of the second part of this paper is included in the abstract of part 1.

The following final results can be derived from the experiments with C₆H₁₂/O₂/N₂:

- I: Because the focus of the work was not on investigating the bulging in the region of the stable detonation, the entire experimental series only produced two values for the ratio α between the static equivalent pressure of the stable detonation and the Chapman-Jouguet pressure p_{CJ} (fields AC15 and AC16 of Table 1). Both values are larger than what had been found for α in a large number of experiments carried out in the past five years (Schildberg (2013 to 2018)). Because these two values are statistically not relevant and because there is no obvious reason why C₆H₁₂/O₂/N₂ mixtures should exhibit a value for α different from the other investigated explosive mixtures, no effort is invested to track down the reason for this deviation and it is assumed that $\alpha = 0.7$ as found in the old tests still holds. Further below, α will be needed to calculate the ratio R between the static equivalent pressure at the location of the DDT and the static equivalent pressure of the stable detonation.
- II: The predetonation distances of the 3 stoichiometric mixtures tested both at $T_{\text{initial}} = 80$ °C and $T_{\text{initial}} = 130$ °C with almost the same initial pressure (to be compared: test 1 and test 5, 19 and 22, 20 and 25) were on the average 26 % longer at the higher initial temperature. This increase is presumably due to the fact that with rising initial temperature the speed of the initial shock front and henceforth also the speed of the unreacted gas behind the initial shock front (see Fig. 7 in Schildberg 2016) rise as well. Consequently, the deflagrative flame has to attain even higher speeds relative to the pipe wall such that the piston represented by the expanding reaction gases finally produces sufficient compression in the unreacted gas ahead of the flame front such that autoignition occurs in the precompressed zone.
- III: For 9 mixtures the ratio between $p_{\text{stat_reflected_stable}}$ and $p_{\text{stat_stable}}$ was measured. All ratios were between 2.06 and 2.9 and the average was 2.38, i.e.

$$p_{\text{stat_reflected_stable}} = 2.38 \cdot p_{\text{stat_stable}}$$

This value confirms the value of 2.4 found in previous investigations (Schildberg 2013, 2015, 2016a, 2018).

- IV: Only for 3 of the 7 tests conducted in short pipes with stoichiometric mixtures (21 vol.-% \leq O₂-concentration in the O₂/N₂ mixture \leq 30 vol.-%) a DDT occurred (tests 22, 32, 35). For scenario 5 the result obtained by averaging over the individual ratios of 4.28, 6.35 and 5.42 is:

$$p_{\text{stat_DDT_short}} = 5.35 \cdot p_{\text{stat_stable}}$$

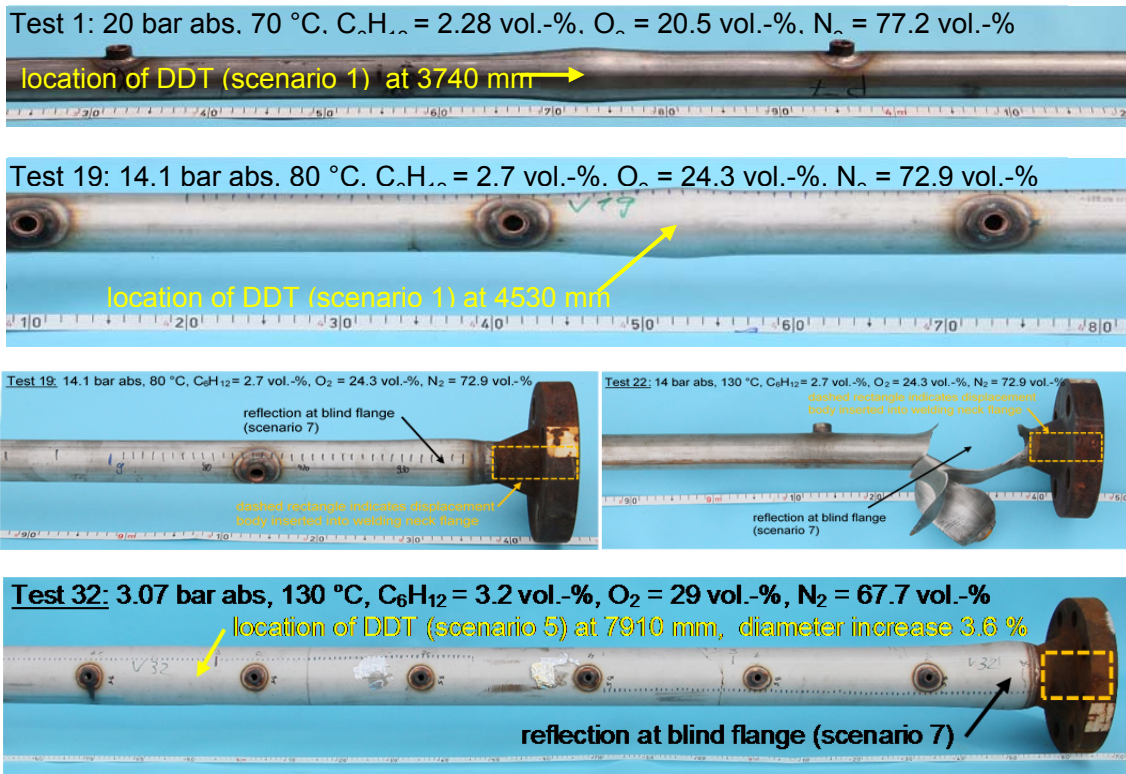


Figure 3: Examples for residual plastic deformations found in the tests with 48.3x2.6 (tests 1, 19 and 22) and 114.3x3.6 (test 32) pipes. Flame propagation was always from left to right, i.e. ignition was always at the left end of the pipes. The steel tape indicates the axial position, i.e. the distance to the ignition source (in units of cm).

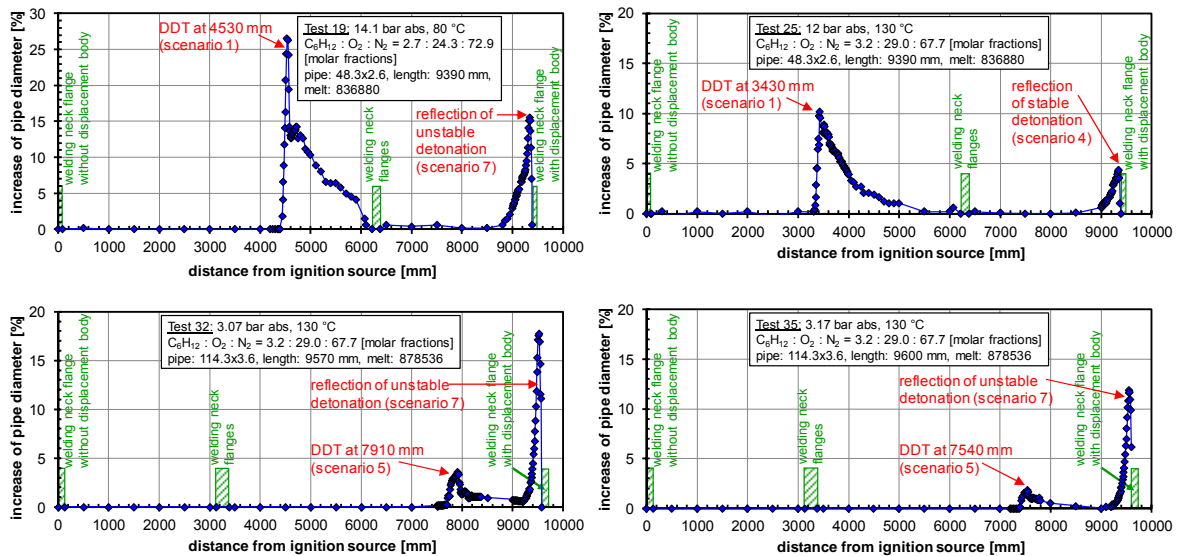


Figure 4: Examples for the increase of the pipe diameters produced by the detonation experiments, plotted over the distance from the ignition source. Further explanations to these special examples are given in the text.

Since R is about 3.7 for the investigated compositions (see further below), this result is in good accordance with the estimation formula for scenario 5 given in Schildberg (2016), i.e. this formula is confirmed:

$$p_{\text{stat_DDT_short}} = 1.5 \cdot R \cdot p_{\text{stat_stable}} = 5.5 \cdot p_{\text{stat_stable}}$$

V: In the short pipe tests nos. 19, 32 and 35 the different ratios found for scenario 7 are 3.55, 10.84 and 8.44. The result obtained by averaging over the three individual ratios is:

$$p_{\text{stat_reflected_unstable}} = 7.6 \cdot p_{\text{stat_stable}}$$

The estimation formula for scenario 7 given in Schildberg (2016) suggests:

$$p_{\text{stat_reflected_unstable}} = 1.5 \cdot 2 \cdot 2.4 \cdot p_{\text{stat_stable}} = 7.2 \cdot p_{\text{stat_stable}}$$

The averaged value is in good accordance with the value predicted by the estimation formula. The systematic scattering of the measured values (the values increase when the location of the DDT gets closer to the blind flange) is explained by Figures 5 and 6. Figure 5 gives the pressure distribution just before the DDT occurs. The estimation formula is based on the blue curve which is slightly simplified. The reality is better approximated by the red curve, which is not flat but drops with increasing distance from the flame front. Therefore scenario 7 will generate higher pressure values when the location of the DDT gets closer to the blind flange ($x/L = 1$), because this will increase the pressure of the unreacted gas ahead of the blind flange at the instant when the detonation front arrives (illustrated in Figure 6).

VI: The variation of the ratio R between the static equivalent pressure at the location of the DDT in the long pipe configuration (scenario 1) and the static equivalent pressure of the stable detonation (scenario 3) as function of C_6H_{12} content is shown in Figure 7. The variation of R along the stoichiometric line is qualitatively identical with what had been found for $H_2/O_2/N_2$, $CH_4/O_2/N_2$ and $C_2H_4/O_2/N_2$. However, the absolute value of R at C_6H_{12} concentrations close to the concentration of C_6H_{12} in stoichiometric C_6H_{12}/air mixtures is about 3.7, and this is less than the corresponding values of R for the other mixtures (ca. 5 for $H_2/O_2/N_2$, ca. 5.5 for $CH_4/O_2/N_2$, ca. 5.6 for $C_2H_4/O_2/N_2$). Once R is known, the short pipe scenarios 5 and 8 can be predicted based on the estimation formulae provided in Schildberg (2016a).

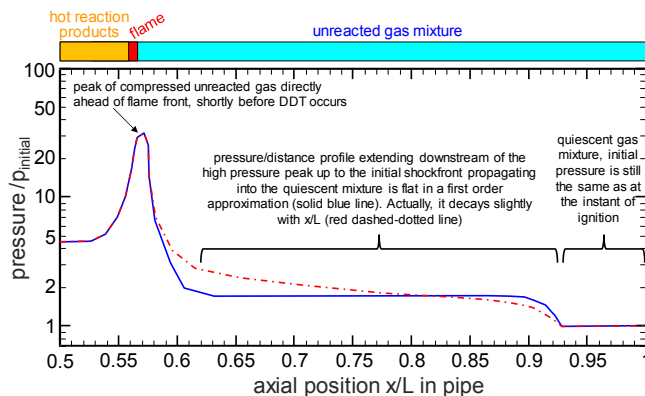
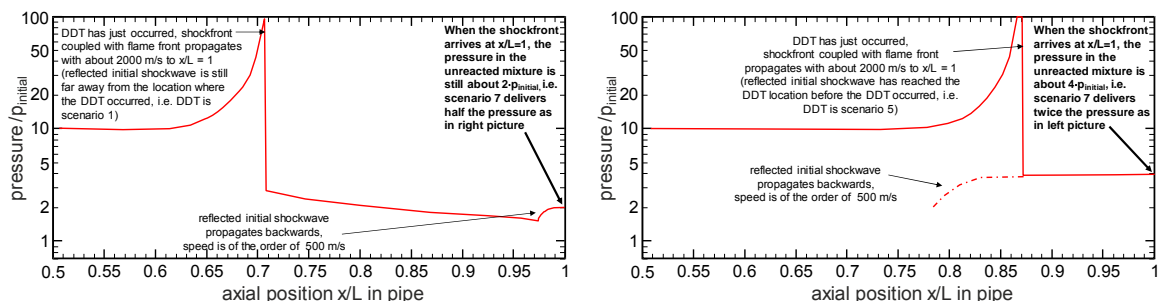


Figure 5: Difference between idealized and true pressure profile of the initial shock wave.



a) DDT occurs in short pipe at large distance from pipe end b) DDT occurs in short pipe close to pipe end

Figure 6: Explanation why – on basis of Figure 5 - the p_{stat} -values of scenario 7 increase when the location of the DDT gets closer to the blind flange of the pipe ($x/L = 1$). All plots show the pressure distribution in the second half of a pipe close to the instant of DDT occurrence.

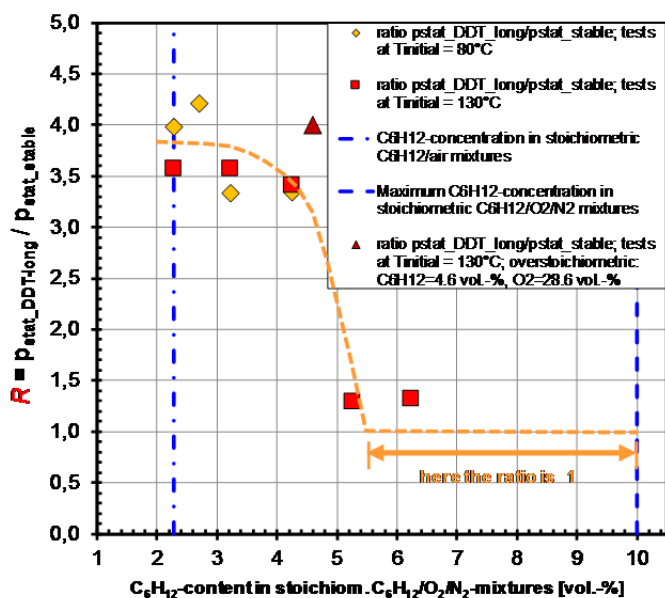


Figure 7: Variation of R in dependence on the C_6H_{12} -content in stoichiometric $C_6H_{12}/O_2/N_2$ mixtures at $T_{initial} = 80\text{ °C}$ and 130 °C . Only the dark-red triangle represents a value for an over-stoichiometric mixture. The orange dashed line is a guide to the eye for the data of the stoichiometric mixtures.

4. Pressure-time diagrams of cyclohexane/ O_2/N_2 -detonations recorded for the run-up stage

An typical example for pressure/time recordings taken for a test is provided by Figure 8. The individual frames show the signals recorded by 15 pressure sensors distributed along the pipe. The positions are printed in the top left corner of each frame and give the distance from the ignition source. The initial shock wave is too small to be visible in the plots, but the development of the zone of precompressed gas directly ahead of the flame front, the detonation peaks, the retonation peaks and the reflected peaks of detonation and retonation can be seen. The topmost frame displays the current of the arc discharge used as ignition source. The instant when the current attains its maximum value is taken as zero point on the time scale. Note that the distance between P4 and P5 is only half of the distance we had between all other neighboring sensors.

Examples for the development of the precompressed zone of unreacted mixture ahead of the flame front in the course of run-up to detonation are shown in Figures 9 to 11. In Figure 9 the pressure peak associated with the precompressed zone of unreacted gas ahead of the flame front is clearly present for the first time at sensor P3.

At sensor P4, which was the last pressure measurement upstream of the DDT location, the peak has attained 470 bar, i.e. at P4 the unreacted gas ahead of the flame front got precompressed by a factor $33.5 = 470\text{ bar}/14\text{ bar}$. In Figure 10 the precompression factor at sensor P5 will be larger than $83.3 = 1000\text{ bar}/12\text{ bar}$ (signal of P5 was cut off at 1000 bar). In Figure 11, which displays the pressures in a short pipe, the precompression factor at P9 is $157 = 500\text{ bar}/3.17\text{ bar}$. In Table 2 all precompression factors found in the experiments are compiled. The values scatter a lot, because the distances between the last pressure sensor upstream of the DDT location and the DDT location vary between 0 and the maximum distance between adjacent pressure sensors, which is 630 mm. Therefore, the maximum precompression factors attained in the precompressed zone of unreacted mixture directly before the DDT occurred will all be larger than the values given in Table 2. When comparing the precompression factors found for stoichiometric cyclohexane/ O_2/N_2 -mixtures in long pipes with those found for stoichiometric $H_2/O_2/N_2$, $CH_4/O_2/N_2$ and $C_2H_4/O_2/N_2$ at oxygen concentrations between 1 and 1.5 times the O_2 -concentration of the stoichiometric combustible/air mixture, the factors of Cyclohexane seem to be only about 50 % to 75 % of the values found for the other mixtures, which are in the range of 70 to 130. A comparison of precompression factors found for stoichiometric mixtures in short pipes is not meaningful due to the relatively small number of tests conducted with C_6H_{12} .

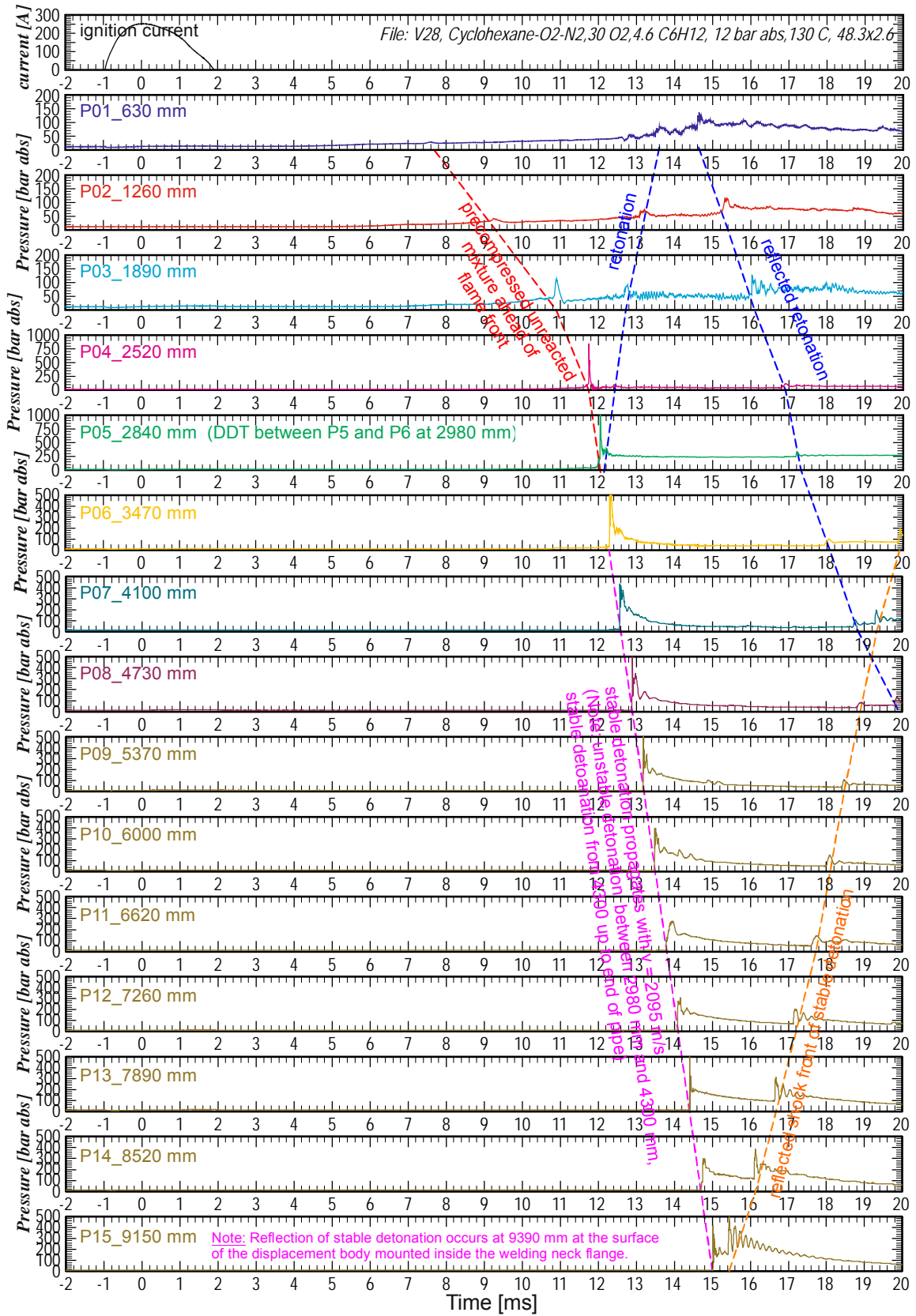
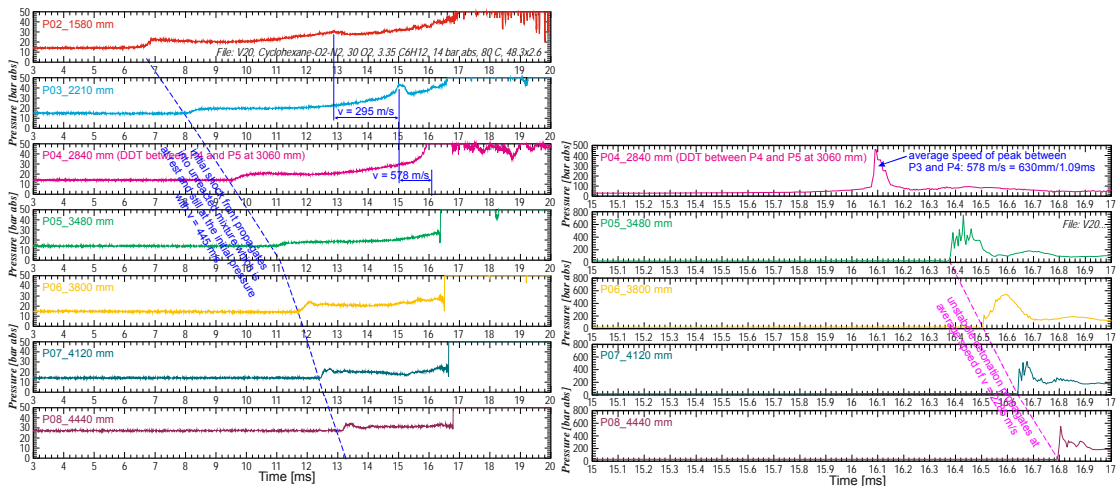


Figure 8: Pressure/time recordings taken for Test 28 by 15 pressure sensors along the pipe. Note that the distance between P4 and P5 is only half of the usual value. The topmost frame displays the ignition current.



a) Initial shock wave is propagating with 445 m/s. Furthermore, the peak associated with the precompressed zone is visible
 b) Signal of sensors 4 to 8 in a scale to show the precompressed zone and the peaks of the unstable detonation.

Figure 9: Pressure-time recordings characterising the run-up to detonation in a long pipe (Test 20).

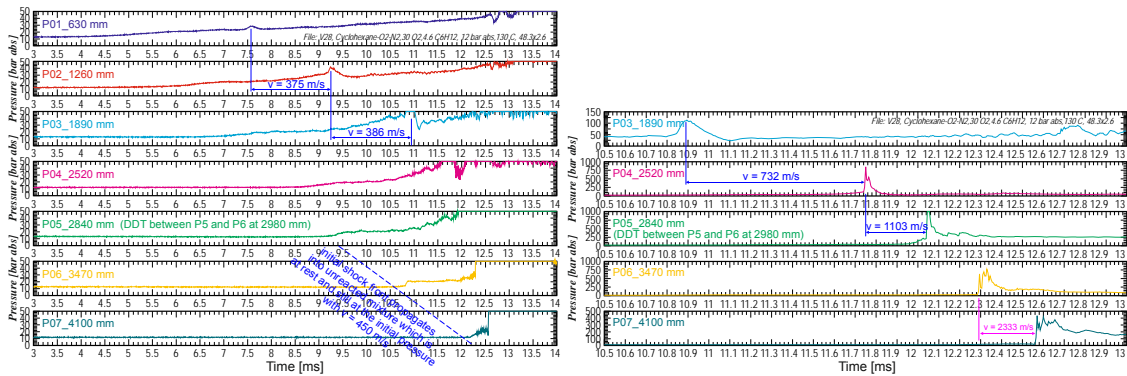


Figure 10: Pressure-time recordings characterising the run-up to detonation in a long pipe (Test 28).

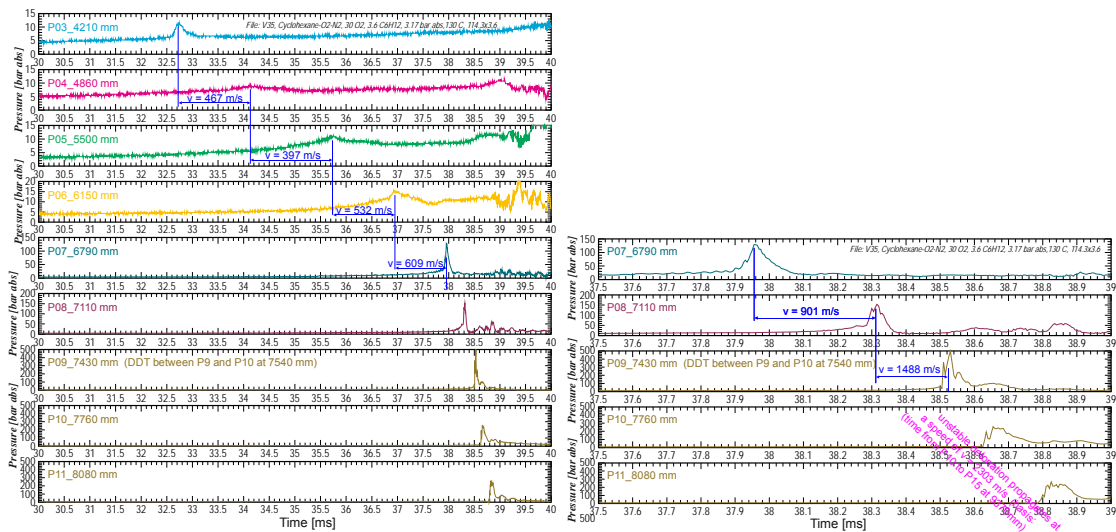


Figure 11: Pressure-time recordings characterising the run-up to detonation in a short pipe (Test 35).